Effect of the Si excess on the structure and the optical properties of Nd-doped Si-rich silicon oxide

C.-H. Liang, O. Debieu, Y.-T. An, L. Khomenkova, J. Cardin*, F. Gourbilleau

CIMAP, UMR CNRS/CEA/ENSICAEN/UCBN, Ensicaen, 6 Bd Maréchal Juin, 14050 Caen Cedex 4, France

Keywords:
Si-rich-silicon oxide
Neodymium
Magnetron sputtering
Refractive index
Infrared absorption
Photoluminescence

A B S T R A C T

Nd-doped Si-rich silicon oxide thin films were produced by radio frequency magnetron co-sputtering of three confocal cathodes: Si, SiO_2, and Nd_2O_3, in pure argon plasma at 500 °C. The microstructure and optical properties of the films were investigated versus silicon excess and post-deposition annealing treatment by means of ellipsometry and Fourier transform infrared spectrometry as well as by the photoluminescence method. A notable emission from Nd^{3+} ions was obtained for the as-deposited sample, while the films annealed at 900 °C showed the highest peak intensity. The maximum emission was observed for the films with 4.7 at% of Si excess.

1. Introduction

During last decade a great research effort has been focused on the development of the Si-based nanostructured materials for photonic application [1–5]. Among them, Si nanoclusters (Si-ncs) embedded in SiO_2 host are widely studied due to an achievement of room-temperature light emission from the blue to the infrared depending on the Si-ncs size [6,7].

Rare-earth (RE) ions possess narrow emission lines and receive more and more interest from the scientists in the world [8]. RE doped silica is a well-known medium for laser application, but its use requires high-power sources to achieve an efficient emission. Considerable attention was paid to silica co-doped with RE ions and Si-ncs since (i) such nanocomposite materials can be pumped using broadband sources due to the spectrally wide absorption of Si-ncs and (ii) Si-ncs are found to be efficient sensitizers of RE ions.

In this regard, the most studied materials are Er-doped Si-rich silicon oxide (SRSO) due to promising application as a source for optical communication. In previous works [9–15] a significant enhancement of photoluminescence (PL) intensity of the intra-4f shell transition of Er^{3+} due to the energy transfer from Si-ncs to RE ions has been demonstrated. The detailed study of the excitation mechanism of Er^{3+} ions showed that the excitation rate depends on the Si-ncs size and becomes higher for the smaller Si-ncs [16].

In the contrast of well-studied Er-SRSO system, other RE ions are not well-addressed. On the contrary to Er^{3+} ions, the doping of SRSO with Nd^{3+} ions is most promising due to overlapping of 4f-shell absorption transitions with the range of intrinsic Si-ncs PL. Moreover, Nd^{3+} ions offer very important light emission in the infrared spectral range at 1.06 and 1.32 μm in a four-level system configuration which avoid re-absorption of the emitted radiation. The benefits of Si-nc sensitizers towards Nd3+ ions was already demonstrated [17,18]. However, its improvement requires a special attention to some critical parameters as the coupling rate between Nd^{3+} ions and Si-ncs as well as the quality of the surrounded host medium aiming significant decrease of the non-radiative channels contribution. In the former case, the coupling rate can be monitored via the Nd^{3+} ions content and the Si excess (Si_{ex}) concentration. The latter has a direct influence on the number of Si-ncs embedded in SiO_2 as well as on the host quality.

In this study, both the structure and the optical properties of Nd-doped SRSO thin films were investigated versus Si_{ex} and the annealing treatment in order to obtain high efficient of Nd^{3+} light emission via energy transfer from Si-ncs toward Nd^{3+} ions.

2. Experimental techniques

The samples were deposited onto p-type silicon wafers by radio frequency magnetron co-sputtering of three confocal cathodes: Si, SiO_2, and Nd_2O_3, in a pure argon plasma. The substrate was rotated during the deposition to ensure a high homogeneity of the film. The deposition temperature and the total plasma pressure were kept at 500 °C and 3 mTorr, respectively. The power density applied on the SiO_2 and the Nd_2O_3 cathodes were fixed at 8.88 and 0.30 W/cm^2, respectively, whereas the power density applied on the Si cathode, P_{Si}, was varied from 0.74 to

* Corresponding author.
E-mail address: julien.cardin@ensicaen.fr (J. Cardin).

2.37 W/cm^2. The deposition time was tuned to achieve the film thickness in the 250–300 nm range for avoiding the effect of the film stresses on the optical parameters [19]. An annealing treatment was performed in a conventional furnace at 900 and 1100 °C during 1 h in a nitrogen flow. Spectroscopic ellipsometry was used to determine the optical constants: thickness and refractive index n of the films. The data were collected by means of a Jobin–Yvon ellipsometer (UVISEL) where the incident light was scanned in the 1.5–4.5 eV range under an incident angle of 66.3°. The fitting of the experimental data was performed using DeltaPsi2 software [20].

The sample's infrared absorption properties were investigated by means of a Nicolet Nexus Fourier transform infrared (FTIR) spectrometer. The spectra were acquired under normal and Brewster angle incidence (65°). The PL spectra were recorded with a photomultiplier tube Hamamatsu (R5108) after dispersion of the PL signal with a Jobin–Yvon TRIAX 180 monochromator using an Ar^+ laser operated at 488 nm which is a non-resonant wavelength for Nd^{3+} excitation. For this study, we focused our PL experiment in the visible-near infrared range (600–1000 nm) to analyze the unique contribution of the RE ions in the de-excitation process [17].

3. Results and discussion

3.1. The Si_{ex} estimation

Fig. 1 displays the evolutions of the refractive index n and the TO_3 peak position of Si–O vibration bond as a function of P_{Si} for as-deposited samples. The n value increases from 1.48 to 1.70 with P_{Si}. According to the effective medium approximation (EMA) and using the Bruggeman model theory [21–23], the O/Si ratio (x) can be determined from the following equation:

$$x = \frac{-36n^4+691n^2+773}{22n^4+665n^2-472} \quad (1)$$

To note that the n value is given at 1.95 eV, and during the deducing of Eq. (1), $n_{a-Si}=4.498$ and $n_{SiO2}=1.457$ are used.

Furthermore, the peak position of the TO_3 mode in Fig. 1 decreases almost linearly with the increased P_{Si}. On the basis of the following equation [24]:

$$x = 0.02\upsilon - 19.3 \quad (2)$$

$\boldsymbol{v}$ is the TO_3 peak position of sample SiO_x, one can obtain the x value. For this pure SiO_2 layer was grown at the same conditions as SRSO-Nd layers and had the same thickness. This approach gives more accurate estimation than the comparison with the TO_3 peak position of SiO_2 ($\sim$1080 cm^{-1}) published elsewhere [25].

Thereafter, Si_{ex} (at%) was calculated from x using the following equation:

$$Si_{ex}(at\%) = \frac{2-x}{2+2x}100 \quad (3)$$

And the results of Si_{ex} estimated from both FTIR and EMA are shown in Fig. 2. It is worth to note that the Si_{ex} values obtained by the two methods are in good agreement within uncertainty.

3.2. Effect of annealing treatment on the microstructure

Fig. 3 shows a typical evolution of the FTIR spectra recorded at the Brewster incidence for films ($P_{Si}=1.33$ W/cm^2) as-deposited and annealed at 900 and 1100 °C. This film was chosen as a typical one to study for its highest emission from Nd^{3+} ions discussed later. The spectra are normalized with respect to the TO_3 phonon mode intensity. It is found that the TO_3 peak position shifts from 1050 to 1080 cm^{-1} with the increasing annealing temperature (T_A). This great shift is explained by the condensation and agglomeration of the Si_{ex} resulting in the formation of Si-ncs [26] at the expense of volumic silica. The evolution of FTIR spectra is a confirmation of the formation of SiO_2 and Si phases via phase separation in the SiO_x host [25]. Moreover, the intensity of the LO_3 peak increases and the intensity of the LO_4–TO_4 pair mode attenuates with the increase of T_A. The former is a signature of the improvement of the Si/SiO_x interface [27], whereas the latter indicates a reduction in disorder of the host.

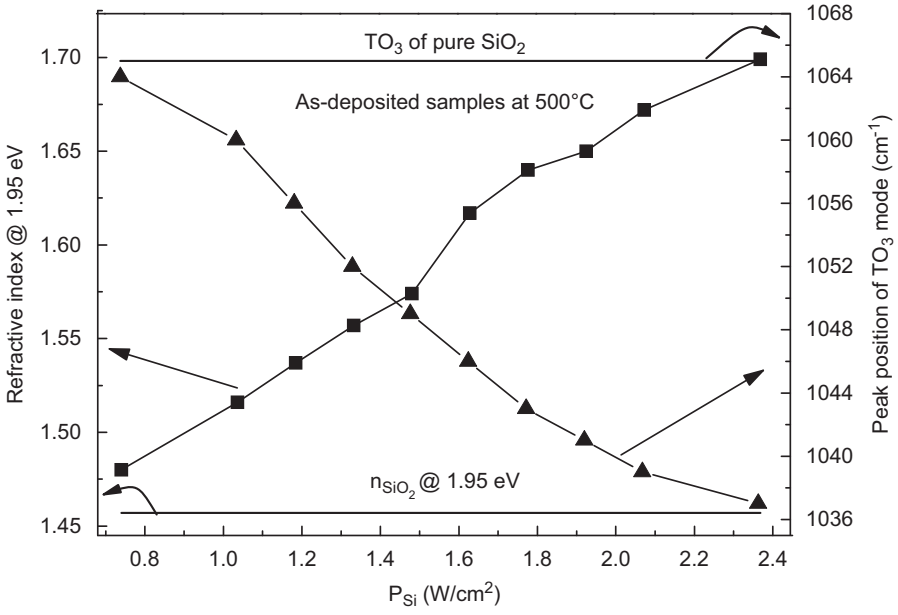

Fig. 1. Evolution of the refractive index n taken at 1.95 eV energy (left axis) and of the TO_3 Si-O peak position (right axis) versus P_{Si} for as-deposited samples. The lines on top and bottom are the TO_3 position (1065 cm^{-1}) and the refractive index n (1.457) for pure SiO_2 grown at the same conditions with the same thickness as SRSO-Nd layers, respectively.

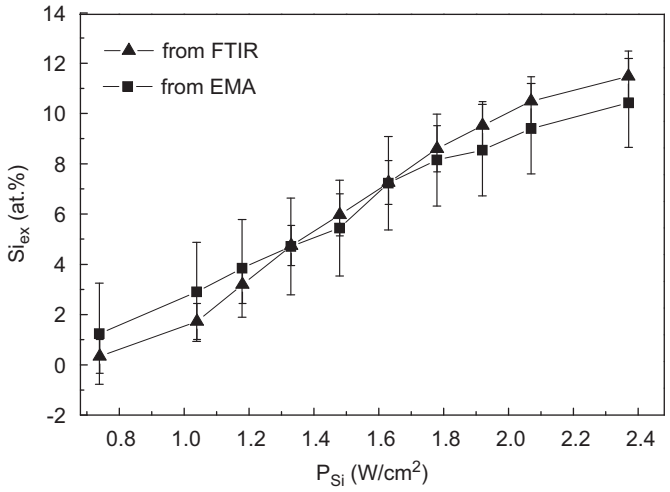

Fig. 2. Evolution of Si_{ex} (at%) as a function of P_{Si} for as-deposited samples.

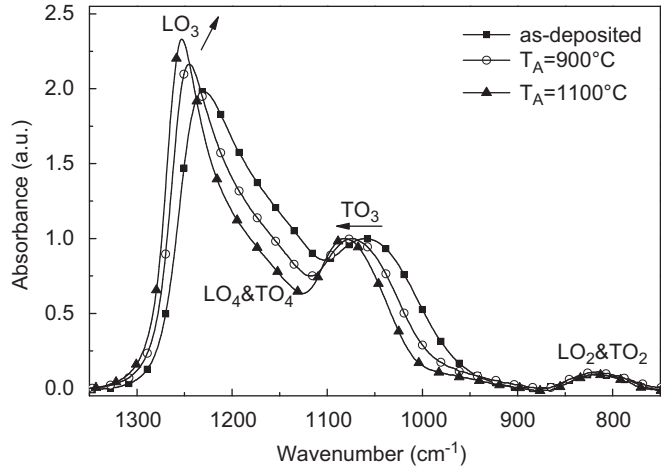

Fig. 3. Typical evolution of the FTIR spectra measured in Brewster incidence for as-deposited and annealed films.

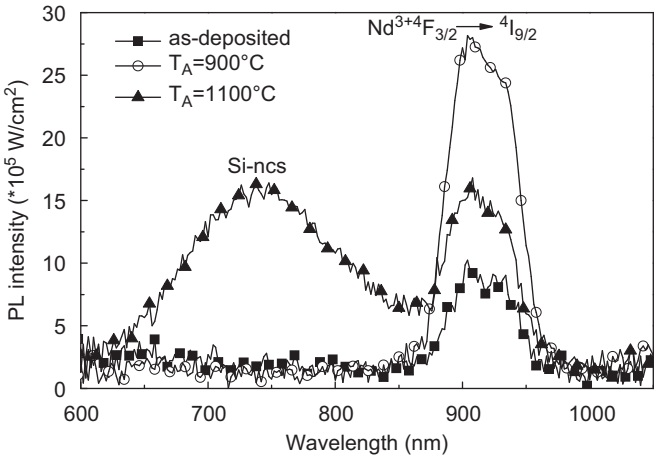

Fig. 4. Typical evolution of the PL spectra of sample with P_{Si}=1.33 W/cm^2 for as-deposited and annealed films.

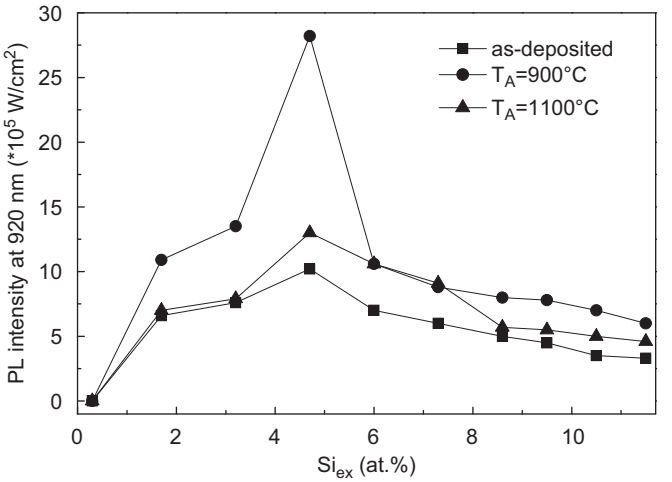

Fig. 5. Evolution of the Nd^{3+} PL intensity at 920 nm as a function of the P_{Si} for as-deposited and annealed films.

3.3. Photoluminescence properties

The film with P_{Si}=1.33 W/cm^2 was once more chosen to demonstrate the evolution of light emission properties versus an annealing treatment. The room temperature PL spectra of sample as-deposited and annealed at 900 and 1100 °C are shown in Fig. 4. It is seen that the sample annealed at 1100 °C emits a broad PL band in the visible domain that can be ascribed to radiative carrier recombination in Si-ncs.

As one can also see from Fig. 4, no emission was detected in this range for both as-deposited and 900 °C-annealed sample. However, this latter FTIR spectrum (Fig. 3) shows a phase separation process and thus the presence of Si-ncs. We conclude that the visible emission is quenched either due to energy transfer or to defect in the host [28]. This assumption is confirmed by the analysis of the Nd^{3+} PL bands (Fig. 4).

In the infrared domain, there are peaks centered at around 920 nm corresponding to the intra-4f shell transition of Nd^{3+} ions from the $^4F_{3/2}$ to the $^4I_{9/2}$ level. The presence of the PL of Nd^{3+} ions after non-resonant excitation at 488 nm confirms the sensitizing effect of Si-ncs toward Nd^{3+} ions. Moreover, the most efficient emission is observed for the sample annealed at 900 °C which corresponds to the best coupling between Si-ncs and Nd^{3+} ions. It is worth to note that a notable emission from Nd^{3+} ions was obtained for the as-deposited sample and this fact can be explained by either formation of Si-ncs during fabrication process or by energy transfer from host defects towards RE ions [19].

In the following part, the effect of Si_{ex} on Nd^{3+} PL properties will be studied as shown in Fig. 5. The Nd^{3+} PL intensity shows first an increase with Si_{ex} for all as-deposited and annealed samples, up to a maximum corresponding to sample with Si_{ex}=4.7% (P_{Si}=1.33 W/cm^2), and then decreases for higher Si_{ex}. This behavior may be explained by two reasons. On one hand, the first increase of Si_{ex} is expected to enhance the density of Si-ncs for an optimized Nd^{3+}:Si-ncs interaction. Further increase of Si_{ex} up to 11.5 at% might lead to increasing the average size of the former Si-ncs at the expense of their density and then of their coupling with Nd^{3+} ions. On the other hand, the Si incorporated into the sample may result in disorder in the host, which will favor the non-radiative channels. Besides in Fig. 5, the samples annealed at 900 °C show the highest PL intensity whatever the Si_{ex}. This observation may be ascribed to the formation of Nd_2O_3 clusters [17] for samples after annealing at high temperature (T_A=1100 °C). To note that there is no peak for sample with Si_{ex}=0.3 at%, possibly because the emission is too weak to be detected for the low Si_{ex}, the Nd^{3+}:Si-ncs distance is too high to allow the energy transfer process.

4. Conclusion

We have investigated the influences of Si_{ex} and T_A on the structure and optical properties of Nd-doped SRSO thin films fabricated by co-sputtering technique. It has been shown that the increase in Si_{ex} improves the Si-ncs coupling to Nd^{3+} ions, and that, it may raise the disorder in layer resulting in the increase of the number of non-radiative channels. In addition, it has been evidenced that the post annealing treatment at 900 and 1100 °C enhances the layer quality favoring the Nd^{3+} PL emission. However, high temperature annealing leads to a decrease of the Nd^{3+} emission due to the coalescence of Si-ncs and/or the formation of Nd_2O_3 cluster. Therefore, both moderate T_A and Si_{ex} are very important to be found with aim to optimize the emission from Nd^{3+} ions. In this study, the sample with Si_{ex}=4.7 at% (P_{Si}=1.33 W/cm^2) shows the highest Nd^{3+} peaks after annealing at 900 °C for 1 h.

Acknowledgments

The authors thank the French National Agency (ANR), which supported this work through the Nanoscience and Nanotechnology program (DAPHNES project ANR-08-NANO-005).

References

[1] A. Polman, B. Min, J. Kalkman, T.J. Kippenberg, K.J. Vahala, Appl. Phys. Lett. 84 (2004) 1037.
[2] A.J. Kenyon, Semicond. Sci. Technol. 20 (2005) R65.
[3] L. Dal Negro, J.H. Yi, J. Michel, L.C. Kimerling, S. Hamel, A. Williamson, G. Galli, IEEE J. Sel. Top. Quantum Electron. 12 (2006) 1628.
[4] M. Fujii, M. Yoshida, Y. Kanzawa, S. Hayashi, K. Yamamoto, Appl. Phys. Lett. 71 (1997) 1198.
[5] A.J. Kenyon, P.F. Trwoga, M. Federighi, C.W. Pitt, J. Phys.: Condens. Matter 6 (1994) L319.
[6] S. Charvet, R. Madelon, F. Gourbilleau, R. Rizk, J. Lumin. 80 (1998) 257.
[7] S. Cueff, C. Labbe´, B. Dierre, F. Fabbri, T. Sekiguchi, X. Portier, R. Rizk, J. Appl. Phys. 108 (2010) 113504.
[8] C.W. Thiel, T. Böttger, R.L. Cone, J. Lumin. 131 (2011) 353.
[9] K. Watanabe, M. Fujii, S. Hayashi, J. Appl. Phys. 90 (2001) 4761.
[10] G. Franzò, S. Bonitelli, D. Pacifici, F. Priolo, F. Iacona, C. Bongiorno, Appl. Phys. Lett. 82 (2003) 3871.
[11] F.D. Pacifici, G. Franzò, F. Priolo, F. Iacona, L.Dal Negro, Phys. Rev. B 67 (2003) 245301.
[12] F. Gourbilleau, M. Levalois, C. Dufour, J. Vicens, R. Rizk, J. Appl. Phys. 95 (2004) 3717.
[13] C. Garcia, P. Pellegrino, Y. Lebour, B. Garrido, F. Gourbilleau, R. Rizk, J. Lumin. 121 (2006) 204.
[14] P. Pellegrino, B. Garrido, J. Arbiol, C. García, Y. Lebour, J.R. Morante, Appl. Phys. Lett. 88 (2006) 121915.
[15] K. Hijazi, R. Rizk, J. Cardin, L. Khomenkova, F. Gourbilleau, J. Appl. Phys. 106 (2009) 024311.
[16] F. Gourbilleau, R. Madelon, C. Dufour, R. Rizk, Opt. Mater. 27 (2005) 868.
[17] O. Debieu, D. Bréard, A. Podhorodecki, G. Zatryb, J. Misiewicz, C. Labbé, J. Cardin, F. Gourbilleau, J. Appl. Phys. 108 (2010) 113114.
[18] D. Bréard, F. Gourbilleau, C. Dufour, R. Rizk, J.-L. Doualan, P. Camy, Mater. Sci. Eng. B. 146 (2008) 179.
[19] S. Cueff, C. Labbé, O. Jambois, B. Garrido, X. Portier, R. Rizk, Nanoscale Res. Lett. 6 (2011) 395.
[20] 〈http://www.horiba.com/scientific/products/ellipsometers/software/〉.
[21] D.E. Aspnes, Thin Solid Films 89 (1982) 249.
[22] E. Dehan, P. Temple-Boyer, R. Henda, J.J. Pedroviejo, E. Scheid, Thin Solid Films 266 (1995) 14.
[23] L. Khomenkova, X. Portier, J. Cardin, F. Gourbilleau, Nanotechnology 21 (2010) 285707.
[24] B.J. Hinds, F. Wang, D.M. Wolfe, C.L. Hinkle, G. Lucovsky, J. Non-Cryst. Solids 227–230 (1998) 507.
[25] S. Charvet, R. Madelon, F. Gourbilleau, R. Rizk, J. Appl. Phys. 85 (1999) 4032.
[26] H. Ono, T. Ikarashi, K. Ando, T. Kitano, J. Appl. Phys. 84 (1998) 6064.
[27] F. Gourbilleau, C. Dufour, M. Levalois, J. Vicens, R. Rizk, C. Sada, F. Enrichi, G. Battaglin, J. Appl. Phys. 94 (2003) 3869.
[28] L. Skuja, J. Non-Cryst. Solids 239 (1998) 16.